

Scattering by Aggregated Fibres Using a Multiple Scattering T-Matrix Approach

Thomas Wriedt*, Roman Schuh**, Adrian Doicu***

(Received: 5 September 2007; in revised form: 12 November 2007; accepted: 14 November 2007; published online: 11 March 2008)

DOI: 10.1002/ppsc.200700022

Abstract

In this paper we consider electromagnetic wave scattering by aggregated fibres using a multiple scattering approach. Scattering by particles of complex shape such as concave particles, torus, or clusters of fibres can not normally be computed using the T-matrix method. In this paper we are proposing a decomposition approach to handle this scattering problem. A scattering particle is

decomposed into a number of basic units and scattering by such an ensemble of basic constituents is computed using a multiple scattering T-matrix approach. The range of validity of this approach is investigated by providing exemplary computation results for single fibres and aggregated fibres.

Keywords: fibre aggregates, scattering, T-matrix

1 Introduction

The crucial advantage of the T-matrix method is that in the T-matrix all properties of the scattering process are contained. Thus with a computed T-matrix orientation averaged scattering can easily be computed. It is also easy to compute multiple scattering by a number of neighboring particles by combining the T-matrices of the single constituents of the ensemble.

Although there was much progress in development of the T-matrix method over the recent decade, there are still some open problems to be solved. Most implementations of the T-matrix method are restricted to rotationally symmetric scattering bodies [1, 2]. There are only a few papers which concern with scattering by particles which lack rotational symmetry. [3, 4, 5]. There are even less papers considering multiple scattering of particles lacking rotational symmetry. As far as we are aware the only re-

sults have been published by Doicu, Wriedt, Eremin [6]. Recent reviews of the literature on the T-matrix method has been published by Mishchenko et al. [7, 8].

Other problems that remain are particles having an extreme aspect ratio such as finite fibres or flat plate like particles. The standard T-matrix method is restricted to particles having an aspect ratio not larger than about 3 to 4. Only special implementations of the T-matrix method making use of discrete sources for expansion of the internal fields can handle large aspect ratios such that scattering by fibres [9] or red blood cells [10] can be computed.

There are still other problems with particles of complex shape such as concave particles, torus shaped particles or clusters of fibres. With clusters of fibres the circumscribed spheres of the constituent fibres would overlap and it would not be possible to compute scattering by such a cluster using the standard multiple scattering approach combining the T-matrices of the individual fibres. Of course, there are alternative methods to compute scattering by particles which do not have these restrictions. These methods include surface based methods such as Multiple Multipole Method (MMP), Discrete Sources Method (DSM), or volume based methods as Volume Integral Equation Method (VIEM), Discrete Dipole Approximation (DDA) and Finite-Difference Time-Domain (FDTD) [11]. With all those methods you would

* Dr. T. Wriedt (corresponding author), Institut für Werkstofftechnik, Badgasteiner Str. 3, 28359 Bremen (Germany).
E-mail: thw@iwt.uni-bremen.de

** R. Schuh, FB4 Verfahrenstechnik, Universität Bremen, Badgasteiner Str 3, 28359 Bremen (Germany).

*** A. Doicu, Institut für Methodik der Fernerkundung, DLR, 82234 Oberpfaffenhofen (Germany).

not get the much searched **T**-matrix and with the volume based methods the scatterer would have to be discretized into volume cells smaller than a tenth of a wavelength which would blow up computational demand.

In a book contribution on particle on surface scattering using the **T**-matrix method we found the geometrical restrictions imposed by having non-overlapping circumscribed spheres can be alleviated [12]. With some amount of overlapping we nonetheless got correct computational results.

With a cluster of two intersecting spheres Ngo et al. [13] did not care about the overlapping circumscribed spheres but the authors did not provide validated results.

In this paper we demonstrate that a scattering particle of complex shape can be decomposed into a number of parts and scattering of this particle can be treated as a multiple scattering problem. We will investigate the applicability of this method with respect to the size of the constituent parts. For validation we will use DDSCAT [14]. First we will shortly outline the multiple scattering **T**-matrix method used in the computational section. In the following section we will show some exemplary computational results to demonstrate the capability of the proposed method.

A short outline of the proposed decomposing method has already been presented in a recent review paper on the Null Field Method with Discrete Sources (NFM-DS) [15].

2 T-Matrix Method

In this section we like to outline the basics of the null-field method for an arbitrary number of nonrotationally symmetric particles by using the translation properties of vector spherical wave functions. Our treatment closely follows the derivation given by Peterson and Ström [16, 17]. The full theory together with all Fortran programs is published in a monograph by Doicu, Wriedt, Eremin [6]. For a full description of the theory the interested reader is referred to this book.

For the purpose of clarity of presentation we will first consider the case of two homogeneous particles in a homogeneous medium with a relative permittivity ϵ_s and a relative permeability μ_s . The scattering geometry of the two particles is shown in Figure 1. The surfaces S_1 and S_2 of the particles are defined with respect to the particle coordinate systems $O_1x_1y_1z_1$ and $O_2x_2y_2z_2$, respectively, while the global coordinate system of the ensemble is denoted by $Oxyz$. The coordinate system $O_1x_1y_1z_1$ is obtained by translating the coordinate system $Oxyz$ through \mathbf{r}_{01} and by rotating the translated coordinate system through the Euler angles α_1, β_1 and γ_1 . Similarly, the coordinate system $O_2x_2y_2z_2$ is obtained by translat-

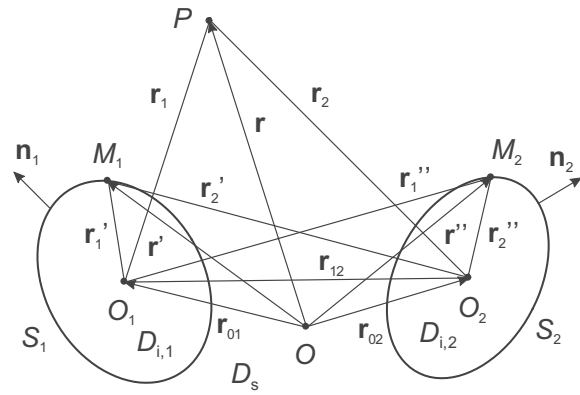


Fig. 1: Geometry of two scattering particles.

ing the coordinate system $Oxyz$ through \mathbf{r}_{02} and by rotating the translated coordinate system through the Euler angles α_2, β_2 and γ_2 . The electromagnetic boundary-value problem for the two scattering particles has the following formulation.

Given the external excitation $\mathbf{E}_e, \mathbf{H}_e$ as an entire solution to the Maxwell equations, find the scattered field $\mathbf{E}_s, \mathbf{H}_s$ and the internal fields $\mathbf{E}_{i,1}, \mathbf{H}_{i,1}$ and $\mathbf{E}_{i,2}, \mathbf{H}_{i,2}$ satisfying the Maxwell equations

$$\begin{aligned}\nabla \times \mathbf{E} &= jk_0\mu\mathbf{H}, \\ \nabla \times \mathbf{H} &= -jk_0\epsilon\mathbf{E}\end{aligned}\quad (1)$$

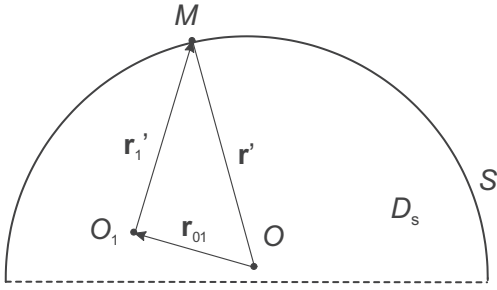
in $D_s, D_{i,1}$, and $D_{i,2}$, the boundary conditions

$$\begin{aligned}\mathbf{n} \times \mathbf{E}_i - \mathbf{n} \times \mathbf{E}_s &= \mathbf{n} \times \mathbf{E}_e, \\ \mathbf{n} \times \mathbf{H}_i - \mathbf{n} \times \mathbf{H}_s &= \mathbf{n} \times \mathbf{H}_e,\end{aligned}\quad (2)$$

on S_1 and on S_2 , and the Silver-Müller radiation condition for the scattered field.

The Stratton-Chu representation theorem [6] for the scattered field \mathbf{E}_s in $D_{i,1}$ and $D_{i,2}$ together with the boundary conditions (2) yield the general null-field equation

$$\begin{aligned}\mathbf{E}_e(\mathbf{r}) + \nabla \times \int_{S_1} \mathbf{e}_{i,1}(\mathbf{r}')g(k_s, \mathbf{r}, \mathbf{r}') dS(\mathbf{r}') \\ + \frac{j}{k_0\epsilon_s} \nabla \times \nabla \times \int_{S_1} \mathbf{h}_{i,1}(\mathbf{r}')g(k_s, \mathbf{r}, \mathbf{r}') dS(\mathbf{r}') \\ + \nabla \times \int_{S_2} \mathbf{e}_{i,2}(\mathbf{r}'')g(k_s, \mathbf{r}, \mathbf{r}'') dS(\mathbf{r}'') \\ + \frac{j}{k_0\epsilon_s} \nabla \times \nabla \times \int_{S_2} \mathbf{h}_{i,2}(\mathbf{r}'')g(k_s, \mathbf{r}, \mathbf{r}'') dS(\mathbf{r}'') \\ = 0, \quad \mathbf{r} \in D_{i,1} \cup D_{i,2}.\end{aligned}$$

Fig. 2: Auxiliary surface Σ .

3 Expansion of the Incident Field

Before we derive the null-field equations, we will present the relation between the expansion coefficients a_v , b_v of the incident field in the global coordinate system $Oxyz$,

$$\mathbf{E}_e(\mathbf{r}) = \sum_v a_v \mathbf{M}_v^1(k_s \mathbf{r}) + b_v \mathbf{N}_v^1(k_s \mathbf{r}),$$

and the expansion coefficients $a_{1,v}$, $b_{1,v}$ of the incident field in the particle coordinate system $O_1 x_1 y_1 z_1$,

$$\mathbf{E}_e(\mathbf{r}_1) = \sum_v a_{1,v} \mathbf{M}_v^1(k_s \mathbf{r}_1) + b_{1,v} \mathbf{N}_v^1(k_s \mathbf{r}_1).$$

For this purpose we choose a sufficiently large surface S enclosing O and O_1 (Figure 2) and in each coordinate system we use the Stratton-Chu representation theorem for the incident field in the interior of S . We obtain

$$\begin{pmatrix} a_v \\ b_v \end{pmatrix} = -\frac{jk_s^2}{\pi} \int_S \left[\mathbf{e}_e(\mathbf{r}') \begin{pmatrix} \mathbf{N}_v^3(k_s \mathbf{r}') \\ \mathbf{M}_v^3(k_s \mathbf{r}') \end{pmatrix} + j\sqrt{\frac{\mu_s}{\epsilon_s}} \mathbf{h}_e(\mathbf{r}') \begin{pmatrix} \mathbf{M}_v^3(k_s \mathbf{r}') \\ \mathbf{N}_v^3(k_s \mathbf{r}') \end{pmatrix} \right] dS(\mathbf{r}'),$$

in the local coordinate system and

$$\begin{pmatrix} a_{1,v} \\ b_{1,v} \end{pmatrix} = -\frac{jk_s^2}{\pi} \int_S \left[\mathbf{e}_e(\mathbf{r}'_1) \begin{pmatrix} \mathbf{N}_v^3(k_s \mathbf{r}'_1) \\ \mathbf{M}_v^3(k_s \mathbf{r}'_1) \end{pmatrix} + j\sqrt{\frac{\mu_s}{\epsilon_s}} \mathbf{h}_e(\mathbf{r}'_1) \begin{pmatrix} \mathbf{M}_v^3(k_s \mathbf{r}'_1) \\ \mathbf{N}_v^3(k_s \mathbf{r}'_1) \end{pmatrix} \right] dS(\mathbf{r}'_1),$$

respectively in the global coordinate system. Using the addition theorem for radiating vector spherical wave functions

$$\begin{bmatrix} \mathbf{M}_v^3(k_s \mathbf{r}'_1) \\ \mathbf{N}_v^3(k_s \mathbf{r}'_1) \end{bmatrix} = \left[(\mathcal{S}_{10}^{\text{rt}})_{\overline{v\mu}} \right] \begin{bmatrix} \mathbf{M}_\mu^3(k_s \mathbf{r}') \\ \mathbf{N}_\mu^3(k_s \mathbf{r}') \end{bmatrix},$$

where the transformation matrix $\mathcal{S}_{10}^{\text{rt}}$ is a product of a translation and a rotation matrix

$$\mathcal{S}_{10}^{\text{rt}} = \mathcal{R}(-\gamma_1, -\beta_1, -a_1) \mathcal{T}^{33}(-k_s \mathbf{r}_{01}), \text{ for } r' > r_{01},$$

and taking into account that the transformation matrix $\mathcal{S}_{10}^{\text{rt}}$ is a block-symmetric matrix, yields the relation of the expansion coefficients of the incident field in the particle coordinate system $O_1 x_1 y_1 z_1$, to the expansion coefficients of the incident field in the global coordinate system $Oxyz$

$$\begin{bmatrix} a_{1,v} \\ b_{1,v} \end{bmatrix} = \left[(\mathcal{S}_{10}^{\text{rt}})_{\overline{v\mu}} \right] \begin{bmatrix} a_\mu \\ b_\mu \end{bmatrix}. \quad (3)$$

The condition $r' > r_{01}$ can always be satisfied in practice by an appropriate choice of the auxiliary surface S , whence, using the identity $\mathcal{T}^{33}(-k_s \mathbf{r}_{01}) = \mathcal{T}^{11}(-k_s \mathbf{r}_{01})$, we see that the transformation matrix $\mathcal{S}_{10}^{\text{rt}}$ is given by

$$\mathcal{S}_{10}^{\text{rt}} = \mathcal{R}(-\gamma_1, -\beta_1, -a_1) \mathcal{T}^{11}(-k_s \mathbf{r}_{01}).$$

4 Two Particle Problem

In this section we like first to derive the \mathbf{T} matrix of the two-particles system. We start with deriving the set of null-field equations needed in the following. Passing from the origin O to the origin O_1 , using the following relations for the Green function

$$\begin{aligned} g(k_s, \mathbf{r}, \mathbf{r}') &= g(k_s, \mathbf{r}_1, \mathbf{r}'_1), \\ g(k_s, \mathbf{r}, \mathbf{r}'') &= g(k_s, \mathbf{r}_1, \mathbf{r}''_1), \end{aligned}$$

and restricting \mathbf{r}_1 to lie on a sphere enclosed in $D_{i,1}$, gives the null-field equations in $D_{i,1}$

$$\begin{aligned}
& \frac{jk_s^2}{\pi} \int_{S_1} \left[\mathbf{e}_{i,1}(\mathbf{r}'_1) \cdot \begin{pmatrix} \mathbf{N}_v^3(k_s \mathbf{r}'_1) \\ \mathbf{M}_v^3(k_s \mathbf{r}'_1) \end{pmatrix} \right. \\
& \left. + j\sqrt{\frac{\mu_s}{\varepsilon_s}} \mathbf{h}_{i,1}(\mathbf{r}'_1) \cdot \begin{pmatrix} \mathbf{M}_v^3(k_s \mathbf{r}'_1) \\ \mathbf{N}_v^3(k_s \mathbf{r}'_1) \end{pmatrix} \right] dS(\mathbf{r}'_1) \\
& + \frac{jk_s^2}{\pi} \int_{S_2} \left[\mathbf{e}_{i,2}(\mathbf{r}'_2) \cdot \begin{pmatrix} \mathbf{N}_v^3(k_s \mathbf{r}'_2) \\ \mathbf{M}_v^3(k_s \mathbf{r}'_2) \end{pmatrix} \right. \\
& \left. + j\sqrt{\frac{\mu_s}{\varepsilon_s}} \mathbf{h}_{i,2}(\mathbf{r}'_2) \cdot \begin{pmatrix} \mathbf{M}_v^3(k_s \mathbf{r}'_2) \\ \mathbf{N}_v^3(k_s \mathbf{r}'_2) \end{pmatrix} \right] dS(\mathbf{r}'_2) \\
& = - \begin{pmatrix} a_{1,v} \\ b_{1,v} \end{pmatrix}, \quad v = 1, 2, \dots,
\end{aligned} \tag{4}$$

where the identities $\mathbf{e}_{i,2}(\mathbf{r}'_2) = \mathbf{e}_{i,2}(\mathbf{r}'_1)$ and $\mathbf{h}_{i,2}(\mathbf{r}'_2) = \mathbf{h}_{i,2}(\mathbf{r}'_1)$ have been used. For the general null-field equation in $D_{i,2}$ we proceed analogously but restrict \mathbf{r}_2 to lie on a sphere enclosed in $D_{i,2}$. We obtain

$$\begin{aligned}
& \frac{jk_s^2}{\pi} \int_{S_1} \left[\mathbf{e}_{i,1}(\mathbf{r}'_1) \cdot \begin{pmatrix} \mathbf{N}_v^3(k_s \mathbf{r}'_2) \\ \mathbf{M}_v^3(k_s \mathbf{r}'_2) \end{pmatrix} \right. \\
& \left. + j\sqrt{\frac{\mu_s}{\varepsilon_s}} \mathbf{h}_{i,1}(\mathbf{r}'_1) \cdot \begin{pmatrix} \mathbf{M}_v^3(k_s \mathbf{r}'_2) \\ \mathbf{N}_v^3(k_s \mathbf{r}'_2) \end{pmatrix} \right] dS(\mathbf{r}'_1) \\
& + \frac{jk_s^2}{\pi} \int_{S_2} \left[\mathbf{e}_{i,2}(\mathbf{r}'_2) \cdot \begin{pmatrix} \mathbf{N}_v^3(k_s \mathbf{r}'_2) \\ \mathbf{M}_v^3(k_s \mathbf{r}'_2) \end{pmatrix} \right. \\
& \left. + j\sqrt{\frac{\mu_s}{\varepsilon_s}} \mathbf{h}_{i,2}(\mathbf{r}'_2) \cdot \begin{pmatrix} \mathbf{M}_v^3(k_s \mathbf{r}'_2) \\ \mathbf{N}_v^3(k_s \mathbf{r}'_2) \end{pmatrix} \right] dS(\mathbf{r}'_2) \\
& = - \begin{pmatrix} a_{2,v} \\ b_{2,v} \end{pmatrix}, \quad v = 1, 2, \dots,
\end{aligned} \tag{5}$$

where, as before, we have taken into account that $\mathbf{e}_{i,1}(\mathbf{r}'_1) = \mathbf{e}_{i,1}(\mathbf{r}'_2)$ and $\mathbf{h}_{i,1}(\mathbf{r}'_1) = \mathbf{h}_{i,1}(\mathbf{r}'_2)$.

The surface fields $\mathbf{e}_{i,1}$, $\mathbf{h}_{i,1}$ and $\mathbf{e}_{i,2}$, $\mathbf{h}_{i,2}$ are the tangential components of the electric and magnetic fields in the domains $D_{i,1}$ and $D_{i,2}$, respectively, and the surface fields approximations can be expressed as linear combinations of regular vector spherical wave functions,

$$\begin{aligned}
& \begin{pmatrix} \mathbf{e}_{i,1}^N(\mathbf{r}'_1) \\ \mathbf{h}_{i,1}^N(\mathbf{r}'_1) \end{pmatrix} = \\
& \sum_{\mu=1}^N c_{1,\mu}^N \begin{pmatrix} \mathbf{n}_1(\mathbf{r}'_1) \times \mathbf{M}_\mu^1(k_{i,1} \mathbf{r}'_1) \\ -j\sqrt{\frac{\varepsilon_{i,1}}{\mu_{i,1}}} \mathbf{n}_1(\mathbf{r}'_1) \times \mathbf{N}_\mu^1(k_{i,1} \mathbf{r}'_1) \end{pmatrix} \\
& + d_{1,\mu}^N \begin{pmatrix} \mathbf{n}_1(\mathbf{r}'_1) \times \mathbf{N}_\mu^1(k_{i,1} \mathbf{r}'_1) \\ -j\sqrt{\frac{\varepsilon_{i,1}}{\mu_{i,1}}} \mathbf{n}_1(\mathbf{r}'_1) \times \mathbf{M}_\mu^1(k_{i,1} \mathbf{r}'_1) \end{pmatrix}
\end{aligned} \tag{6}$$

and

$$\begin{aligned}
& \begin{pmatrix} \mathbf{e}_{i,2}^N(\mathbf{r}'_2) \\ \mathbf{h}_{i,2}^N(\mathbf{r}'_2) \end{pmatrix} = \\
& \sum_{\mu=1}^N c_{2,\mu}^N \begin{pmatrix} \mathbf{n}_2(\mathbf{r}'_2) \times \mathbf{M}_\mu^1(k_{i,2} \mathbf{r}'_2) \\ -j\sqrt{\frac{\varepsilon_{i,2}}{\mu_{i,2}}} \mathbf{n}_2(\mathbf{r}'_2) \times \mathbf{N}_\mu^1(k_{i,2} \mathbf{r}'_2) \end{pmatrix} \\
& + d_{2,\mu}^N \begin{pmatrix} \mathbf{n}_2(\mathbf{r}'_2) \times \mathbf{N}_\mu^1(k_{i,2} \mathbf{r}'_2) \\ -j\sqrt{\frac{\varepsilon_{i,2}}{\mu_{i,2}}} \mathbf{n}_2(\mathbf{r}'_2) \times \mathbf{M}_\mu^1(k_{i,2} \mathbf{r}'_2) \end{pmatrix}
\end{aligned} \tag{7}$$

Inserting these expansions (6) and (7) into the null-field equations (4) and (5), using the addition theorem for vector spherical wave functions

$$\begin{bmatrix} \mathbf{M}_v^3(k_s \mathbf{r}'_2) \\ \mathbf{N}_v^3(k_s \mathbf{r}'_2) \end{bmatrix} = \left[\left(\tilde{\mathcal{S}}_{12}^{\text{trr}} \right)_{\overline{v\mu}} \right] \begin{bmatrix} \mathbf{M}_\mu^1(k_s \mathbf{r}'_1) \\ \mathbf{N}_\mu^1(k_s \mathbf{r}'_1) \end{bmatrix},$$

with

$$\tilde{\mathcal{S}}_{12}^{\text{trr}} = \mathcal{R}(-\gamma_1, -\beta_1, -a_1) \mathcal{T}^{31}(k_s \mathbf{r}_{12}) \mathcal{R}(a_2, \beta_2, \gamma_2),$$

for $r'_2 < r_{12}$,

and

$$\begin{bmatrix} \mathbf{M}_v^3(k_s \mathbf{r}'_2) \\ \mathbf{N}_v^3(k_s \mathbf{r}'_2) \end{bmatrix} = \left[\left(\tilde{\mathcal{S}}_{21}^{\text{trr}} \right)_{\overline{v\mu}} \right] \begin{bmatrix} \mathbf{M}_\mu^1(k_s \mathbf{r}'_1) \\ \mathbf{N}_\mu^1(k_s \mathbf{r}'_1) \end{bmatrix},$$

with

$$\tilde{\mathcal{S}}_{21}^{\text{trr}} = \mathcal{R}(-\gamma_2, -\beta_2, -a_2) \mathcal{T}^{31}(-k_s \mathbf{r}_{12}) \mathcal{R}(a_1, \beta_1, \gamma_1),$$

for $r'_1 < r_{12}$,

and taking into account the transformation rule for the incident field coefficients (3), yields the system of matrix equations

$$\begin{aligned}
& \mathbf{Q}_1^{31}(k_s, k_{i,1}) \mathbf{i}_1 + \tilde{\mathcal{S}}_{12}^{\text{trr}} \mathbf{Q}_2^{11}(k_s, k_{i,2}) \mathbf{i}_2 = -\mathcal{S}_{10}^{\text{rt}} \mathbf{e}, \\
& \tilde{\mathcal{S}}_{21}^{\text{trr}} \mathbf{Q}_1^{11}(k_s, k_{i,1}) \mathbf{i}_1 + \mathbf{Q}_2^{31}(k_s, k_{i,2}) \mathbf{i}_2 = -\mathcal{S}_{20}^{\text{rt}} \mathbf{e},
\end{aligned} \tag{8}$$

where $\mathbf{i}_1 = [c_{1,\mu}^N, d_{1,\mu}^N]^T$, $\mathbf{i}_2 = [c_{2,\mu}^N, d_{2,\mu}^N]^T$, and as usually, $\mathbf{e} = [a_v, b_v]^T$ is the vector containing the expansion coefficients of the incident field in the global coordinate system. Further, defining the scattered field coefficients,

$$\begin{aligned}
& \mathbf{s}_1 = \mathbf{Q}_1^{11}(k_s, k_{i,1}) \mathbf{i}_1, \\
& \mathbf{s}_2 = \mathbf{Q}_2^{11}(k_s, k_{i,2}) \mathbf{i}_2,
\end{aligned}$$

and introducing the individual transition matrices,

$$\begin{aligned}\mathbf{T}_1 &= -\mathbf{Q}_1^{11}(k_s, k_{i,1}) [\mathbf{Q}_1^{31}(k_s, k_{i,1})]^{-1}, \\ \mathbf{T}_2 &= -\mathbf{Q}_2^{11}(k_s, k_{i,2}) [\mathbf{Q}_2^{31}(k_s, k_{i,2})]^{-1},\end{aligned}$$

we can rewrite the matrix system (8) as

$$\begin{aligned}\mathbf{s}_1 - \mathbf{T}_1 \tilde{\mathcal{S}}_{12}^{\text{rtr}} \mathbf{s}_2 &= \mathbf{T}_1 \mathcal{S}_{10}^{\text{rt}} \mathbf{e}, \\ \mathbf{s}_2 - \mathbf{T}_2 \tilde{\mathcal{S}}_{21}^{\text{rtr}} \mathbf{s}_1 &= \mathbf{T}_2 \mathcal{S}_{20}^{\text{rt}} \mathbf{e},\end{aligned}$$

and thus find the solutions for the scattered field coefficients

$$\begin{aligned}\mathbf{s}_1 &= \mathbf{T}_1 \left(\mathbf{I} - \tilde{\mathcal{S}}_{12}^{\text{rtr}} \mathbf{T}_2 \tilde{\mathcal{S}}_{21}^{\text{rtr}} \mathbf{T}_1 \right)^{-1} \left(\mathcal{S}_{10}^{\text{rt}} + \tilde{\mathcal{S}}_{12}^{\text{rtr}} \mathbf{T}_2 \mathcal{S}_{20}^{\text{rt}} \right), \\ \mathbf{s}_2 &= \mathbf{T}_2 \left(\mathbf{I} - \tilde{\mathcal{S}}_{21}^{\text{rtr}} \mathbf{T}_1 \tilde{\mathcal{S}}_{12}^{\text{rtr}} \mathbf{T}_2 \right)^{-1} \left(\mathcal{S}_{20}^{\text{rt}} + \tilde{\mathcal{S}}_{21}^{\text{rtr}} \mathbf{T}_1 \mathcal{S}_{10}^{\text{rt}} \right).\end{aligned}\quad (9)$$

To compute the \mathbf{T} matrix of the two-particles system and to derive a scattered-field expansion centered at the origin $Oxyz$ of the global coordinate system we use the Stratton-Chu representation theorem for the scattered field \mathbf{E}_s in D_s . In the exterior of a sphere enclosing the two particles, the expansion of the approximate scattered field \mathbf{E}_s^N in terms of radiating vector spherical wave functions reads as

$$\mathbf{E}_s^N(\mathbf{r}) = \sum_{v=1}^N f_v^N \mathbf{M}_v^3(k_s \mathbf{r}) + g_v^N \mathbf{N}_v^3(k_s \mathbf{r}), \quad (10)$$

where the expansion coefficients $\mathbf{s} = [f_v^N, g_v^N]^T$ are given by

$$\begin{aligned}\begin{pmatrix} f_v^N \\ g_v^N \end{pmatrix} &= \frac{jk_s^2}{\pi} \int_{S_1} \left[\mathbf{e}_{i,1}^N(\mathbf{r}_1) \begin{pmatrix} \mathbf{N}_v^1(k_s \mathbf{r}') \\ \mathbf{M}_v^1(k_s \mathbf{r}') \end{pmatrix} \right. \\ &+ j \sqrt{\frac{\mu_s}{\varepsilon_s}} \mathbf{h}_{i,1}^N(\mathbf{r}_1) \begin{pmatrix} \mathbf{M}_v^1(k_s \mathbf{r}') \\ \mathbf{N}_v^1(k_s \mathbf{r}') \end{pmatrix} \left. \right] dS(\mathbf{r}_1) \\ &+ \frac{jk_s^2}{\pi} \int_{S_2} \left[\mathbf{e}_{i,2}^N(\mathbf{r}_2) \begin{pmatrix} \mathbf{N}_v^1(k_s \mathbf{r}'') \\ \mathbf{M}_v^1(k_s \mathbf{r}'') \end{pmatrix} \right. \\ &+ j \sqrt{\frac{\mu_s}{\varepsilon_s}} \mathbf{h}_{i,2}^N(\mathbf{r}_2) \begin{pmatrix} \mathbf{M}_v^1(k_s \mathbf{r}'') \\ \mathbf{N}_v^1(k_s \mathbf{r}'') \end{pmatrix} \left. \right] dS(\mathbf{r}_2).\end{aligned}\quad (11)$$

Finally, using the addition theorem for the regular vector spherical wave functions,

$$\begin{bmatrix} \mathbf{M}_v^1(k_s \mathbf{r}') \\ \mathbf{N}_v^1(k_s \mathbf{r}') \end{bmatrix} = \left[(\mathcal{S}_{01}^{\text{tr}})_{\overline{v\mu}} \right] \begin{bmatrix} \mathbf{M}_\mu^1(k_s \mathbf{r}'_1) \\ \mathbf{N}_\mu^1(k_s \mathbf{r}'_1) \end{bmatrix},$$

with the transformation matrix $\mathcal{S}_{01}^{\text{tr}}$ given as a product of a translation and a rotation matrix

$$\mathcal{S}_{01}^{\text{tr}} = \mathcal{T}^{11}(k_s \mathbf{r}_{01}) \mathcal{R}(a_1, \beta_1, \gamma_1),$$

and

$$\begin{bmatrix} \mathbf{M}_v^1(k_s \mathbf{r}'') \\ \mathbf{N}_v^1(k_s \mathbf{r}'') \end{bmatrix} = \left[(\mathcal{S}_{02}^{\text{tr}})_{\overline{v\mu}} \right] \begin{bmatrix} \mathbf{M}_\mu^1(k_s \mathbf{r}'_2) \\ \mathbf{N}_\mu^1(k_s \mathbf{r}'_2) \end{bmatrix},$$

with

$$\mathcal{S}_{02}^{\text{tr}} = \mathcal{T}^{11}(k_s \mathbf{r}_{02}) \mathcal{R}(a_2, \beta_2, \gamma_2),$$

we obtain the expansion coefficients of the scattered field

$$\begin{aligned}\mathbf{s} &= \mathcal{S}_{01}^{\text{tr}} \mathbf{Q}_1^{11}(k_s, k_{i,1}) \mathbf{i}_1 + \mathcal{S}_{02}^{\text{tr}} \mathbf{Q}_2^{11}(k_s, k_{i,2}) \mathbf{i}_2 \\ &= \mathcal{S}_{01}^{\text{tr}} \mathbf{s}_1 + \mathcal{S}_{02}^{\text{tr}} \mathbf{s}_2,\end{aligned}\quad (12)$$

where $\mathbf{s} = [f_v^N, g_v^N]^T$ is the vector containing the expansion coefficients of the scattered field in the global coordinate system. Combining (9) and (12), and using the identities $\mathcal{S}_{20}^{\text{tr}} (\mathcal{S}_{10}^{\text{rt}})^{-1} = \mathcal{S}_{21}^{\text{rtr}}$ and $\mathcal{S}_{10}^{\text{rt}} (\mathcal{S}_{20}^{\text{tr}})^{-1} = \mathcal{S}_{12}^{\text{rtr}}$, yields the \mathbf{T} matrix [16]

$$\begin{aligned}\mathbf{T} &= \mathcal{S}_{01}^{\text{tr}} \mathbf{T}_1 \left(\mathbf{I} - \tilde{\mathcal{S}}_{12}^{\text{rtr}} \mathbf{T}_2 \tilde{\mathcal{S}}_{21}^{\text{rtr}} \mathbf{T}_1 \right)^{-1} \left(\mathbf{I} + \tilde{\mathcal{S}}_{12}^{\text{rtr}} \mathbf{T}_2 \mathcal{S}_{21}^{\text{rtr}} \right) \mathcal{S}_{10}^{\text{rt}} \\ &+ \mathcal{S}_{02}^{\text{tr}} \mathbf{T}_2 \left(\mathbf{I} - \tilde{\mathcal{S}}_{21}^{\text{rtr}} \mathbf{T}_1 \tilde{\mathcal{S}}_{12}^{\text{rtr}} \mathbf{T}_2 \right)^{-1} \\ &\times \left(\mathbf{I} + \tilde{\mathcal{S}}_{21}^{\text{rtr}} \mathbf{T}_1 \mathcal{S}_{12}^{\text{rtr}} \right) \mathcal{S}_{20}^{\text{rt}},\end{aligned}\quad (13)$$

where the explicit expressions of the transformation matrices $\mathcal{S}_{21}^{\text{rtr}}$ and $\mathcal{S}_{12}^{\text{rtr}}$ are given by

$$\mathcal{S}_{12}^{\text{rtr}} = \mathcal{R}(-\gamma_1, -\beta_1, -a_1) \mathcal{T}^{11}(k_s \mathbf{r}_{12}) \mathcal{R}(a_2, \beta_2, \gamma_2),$$

and

$$\mathcal{S}_{21}^{\text{tr}} = \mathcal{R}(-\gamma_2, -\beta_2, -a_2) \mathcal{T}^{11}(-k_s \mathbf{r}_{12}) \mathcal{R}(a_1, \beta_1, \gamma_1),$$

respectively, where \mathcal{T} and \mathcal{R} are defined in Appendix B of Doicu, Wriedt, Eremin [6]. Equation (13) gives the system transition matrix \mathbf{T} in terms of the individual transition matrices \mathbf{T}_1 and \mathbf{T}_2 , and the transformation matrices \mathcal{S} and $\tilde{\mathcal{S}}$. The transformation matrices \mathcal{S} and $\tilde{\mathcal{S}}$ involve translations of the regular and radiating vector spherical wave functions, respectively, and geometric constraints are introduced by the $\tilde{\mathcal{S}}$ matrices.

5 \mathcal{N} Particle Generalization

The generalization of the \mathbf{T} -matrix relation to a system with more than two constituent particles is presented next. The system of matrix equations consists in the null-field equations in the interior of all particles S_l ,

$$\mathbf{s}_l - \mathbf{T}_l \sum_{p \neq l}^N \tilde{\mathcal{S}}_{lp}^{\text{tr}} \mathbf{s}_p = \mathbf{T}_l \mathcal{S}_{l0}^{\text{tr}} \mathbf{e}, \text{ for } l = 1, 2, \dots, \mathcal{N}, \quad (14)$$

and the matrix equation corresponding to the scattered field representation

$$\mathbf{s} = \sum_{l=1}^N \mathcal{S}_{0l}^{\text{tr}} \mathbf{s}_l. \quad (15)$$

In a practical computer implementation it is appropriate to consider the global matrix \mathbf{A} with block-matrix components give by

$$\begin{aligned} \mathbf{A}^{ll} &= \mathbf{I}, \quad l = 1, 2, \dots, \mathcal{N}, \\ \mathbf{A}^{lp} &= -\mathbf{T}_l \tilde{\mathcal{S}}_{lp}^{\text{tr}}, \quad l \neq p, \quad l, p = 1, 2, \dots, \mathcal{N}, \end{aligned}$$

and to express the solution to the system of matrix equations (14) as

$$\mathbf{s}_l = \left(\sum_{p=1}^N \mathcal{A}^{lp} \mathbf{T}_p \mathcal{S}_{p0}^{\text{tr}} \right) \mathbf{e}, \quad l = 1, 2, \dots, \mathcal{N}, \quad (16)$$

where \mathcal{A} stands for \mathbf{A}^{-1} , and \mathcal{A}^{lp} , $l, p = 1, 2, \dots, \mathcal{N}$, are the block-matrix components of \mathcal{A} . In view of the scattered field representation (15), the system \mathbf{T} -matrix becomes

$$\mathbf{T} = \sum_{l=1}^{\mathcal{N}} \sum_{p=1}^{\mathcal{N}} \mathcal{S}_{0l}^{\text{tr}} \mathcal{A}^{lp} \mathbf{T}_p \mathcal{S}_{p0}^{\text{tr}},$$

and this transition matrix can be used to compute the scattering characteristics for fixed or random orientations of an ensemble of arbitrarily shaped nonrotationally symmetric particles.

From the \mathbf{T} -matrix the scattered field (10) can be computed and all other scattering quantities. Especially for plotting the scattering diagrams shown in the next section we compute the differential scattering cross section (DSCS) for p and s incident polarization from the far field pattern \mathbf{E}_{∞} that is the vector field given on the unit sphere:

$$\text{DSCS} = |\mathbf{E}_{\infty}|^2$$

6 Simulation Results

The following simulation results were obtained using the \mathbf{T} -matrix program included on CD with the monograph by Doicu, Wriedt, Eremin [6]. The first computational step involves the calculation of the individual \mathbf{T} -matrix of the basic cylinder by using the TAXSYM code. The individual \mathbf{T} -matrices are then used to compute the \mathbf{T} -matrix of the long fibres using multiple scattering with the TMULT routine. In our exemplary simulations for fibres we additionally use the program DDSCAT by Draine and Flatau [14] for the numerical comparison of our results. This program utilizes the method of Discrete Dipole Approximation (DDA) for the computation of the light scattering by arbitrary shaped particles. The modelling of the fibres is done by the included pre-defined shape routine for a cylinder. For the attached fibres we generate a shape file as input for DDSCAT with a special MATLAB algorithm [18].

For the analysis of the deviations in the DSCS (differential scattering cross section) between the different configurations we use a root mean square value (RMS) which is defined by

$$\begin{aligned} \text{RMS}(\text{DSCS}_1, \text{DSCS}_2) &= \\ &= \sqrt{\frac{1}{181} \sum_{i=1}^{181} (\log \text{DSCS}_1(i) - \log \text{DSCS}_2(i))^2}, \end{aligned}$$

where DSCS_1 and DSCS_2 denote the respective DSCS in the scattering plane ($0^\circ < \theta < 180^\circ$, $\varphi = 0^\circ$).

6.1 Single Fibres

The scattering object which is to be investigated in this paper consists of two attached cylindrical fibres. In order to understand from where exactly the sources of potential errors arise in the computation of the light scattering by two attached fibres, we first investigate the scattering by single fibres composed of shorter basic cylindrical parts. The fibre is modelled as a cylinder with length to diameter aspect ratio of 8:1. The fibre has a refractive index of $1.5+0.0i$. The size of the fibre is varied in a wide range where the aspect ratio is kept constant to 8:1. The smallest size of the fibre is $kr = 0.25$, where $k = 2\pi/\lambda$ is the wavenumber and r is the radius of the fibre. The wavelength of the incident plane wave is chosen to be $\lambda = 2\pi/10$.

We consider different decompositions of the single fibre. Depending on the configuration, the fibre is composed of different numbers of basic elements. In the first configuration the fibre is decomposed into eight single basic cylinders with the aspect ratio of 1:1, called 'T-Matrix 8'. In the second configuration the fibre consists of four single basic cylinders of 2:1, called 'T-Matrix 4'. The third configuration shows two basic cylinders with the aspect ratio of 4:1, called 'T-Matrix 2'. The fourth configuration 'T-Matrix' is simply one cylinder representing the original fibre. The used configurations are shown in Figure 3. For each configuration we use discrete sources for the expansion of internal fields that are placed along the axis of the individual basic cylinders. Without using discrete sources the computation of the T-matrix for the elongated cylinders would not be possible as the chosen aspect ratio is quite high. The light always is incident parallel to the z axis. In each configuration the fibre is aligned along the z axis.

In Figure 4 there is shown a comparison of the DSCS for the five different methods of computation. In the figure the simulation results are shown for both, the s-polarized and for p-polarized incident wave. The size parameter of the fibre is $kd = 2.0$. There is excellent agreement comparing the DSCSs of the five different computations for the s-polarization. For the p-polarization there are minor deviations in the range of the scat-

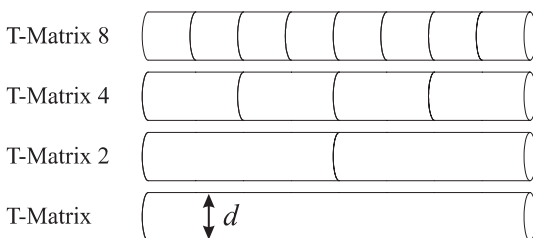


Fig. 3: Different decompositions of a fibre.

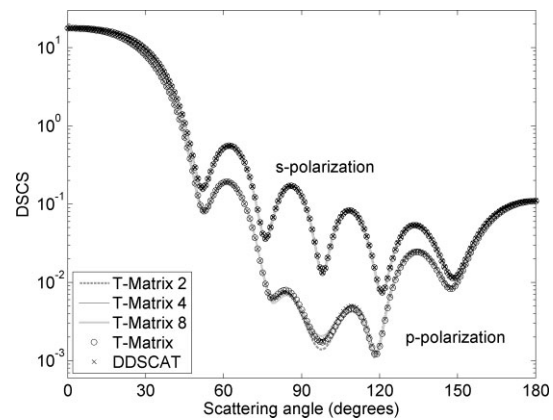


Fig. 4: DSCS for different configurations of the fibre. The size parameter of the fibre is $kd = 2.0$. The scattering results for the s- and the p-polarization is shown.

tering angle between 90° and 120° . These deviations mainly apply to the configurations of 'T-Matrix 2' and 'T-Matrix 8'.

The RMS error dependent on the size parameter is shown in Figure 5. The RMS error is defined by the deviations relative to the original configuration 'T-Matrix', which is the configuration without any decomposition. It can be seen that up to a size parameter of $kd = 2.0$ the results for the different configurations show good agreement. The results for the s-polarization are slightly better compared to the p-polarization. The configuration 'T-Matrix 8' with a decomposition into 8 parts shows the highest deviations. Nevertheless, the RMS error is acceptable up to a size parameter of $kd = 2.0$. For a size parameter higher than 2.0 the RMS error is strongly increasing for both polarizations.

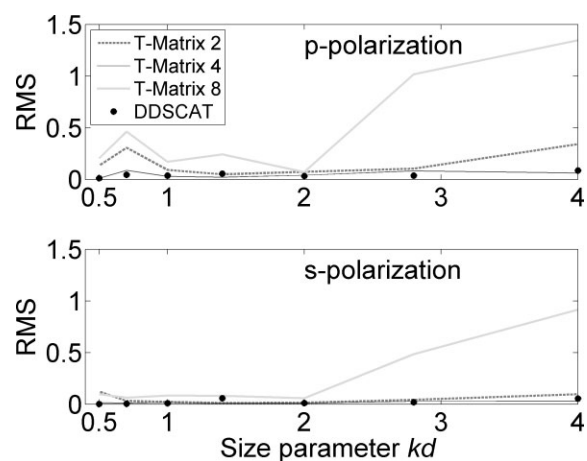


Fig. 5: RMS error depending on the size parameter kd for different configurations of a single fibre compared to the original 'T-Matrix' configuration. Top: The RMS for the p-polarization is shown. Bottom: The RMS for the s-polarization is shown.

The other configurations of decomposition, namely the 'T-Matrix 2' and 'T-Matrix 4' show only small deviations. Especially, the configuration 'T-Matrix 4' shows excellent agreement for all considered size parameters.

The RMS error comparing DDSCAT and 'T-Matrix' computations in Figure 5 is negligibly small and is not leading to visible differences in the computed scattering distribution (DSCS). Thus, the simulation results obtained with DDSCAT ensure the validity of the **T**-matrix calculations.

6.2 Aggregated Fibres

As an example for scattering by aggregated fibres using decomposition we would like to present the computed scattering results for two orthogonally attached fibres like shown in Figure 6. It can be clearly seen that the intersection volume of the circumscribing spheres is strongly reduced by using decomposition of the fibres.

Both fibres have a length/diameter aspect ratio of 9:1. The first fibre has a refractive index of $m_1 = 1.5$. The second fibre has a refractive index of $m_2 = 1.3$. The fibres are attached at the center of the first fibre. The second fibre is shifted $2.5d$ from the end of the fibre. The plane wave is incident in the z -direction. The scattering plane lies in the x_0z -plane. The model of the two fibres is depicted in Figure 7.

The results of the scattering simulations are depicted in Figure 8. In this example the size parameter is $kd = 2.0$. Using the wavelength $\lambda = 0.628\text{nm}$, the diameter of each of the fibres is $d = 0.2\mu\text{m}$ and the length is $l = 1.8\mu\text{m}$. The comparison of the **T**-matrix with a DDA computation done with the program DDSCAT shows very good agreement in the DSCS.

The RMS error which is computed from the deviations between the **T**-matrix and the DDA computations is

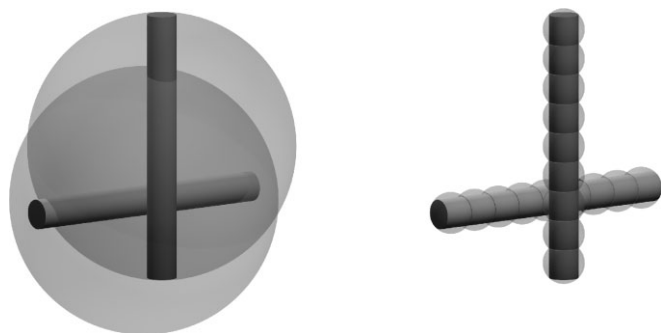


Fig. 6: Model of two attached fibres with the circumscribing spheres. Left: The circumscribing spheres of the two fibres show a large intersection volume. Right: Decomposition of each of the fibres into nine cylinders leads to small circumscribing spheres. The intersection volume is strongly reduced.

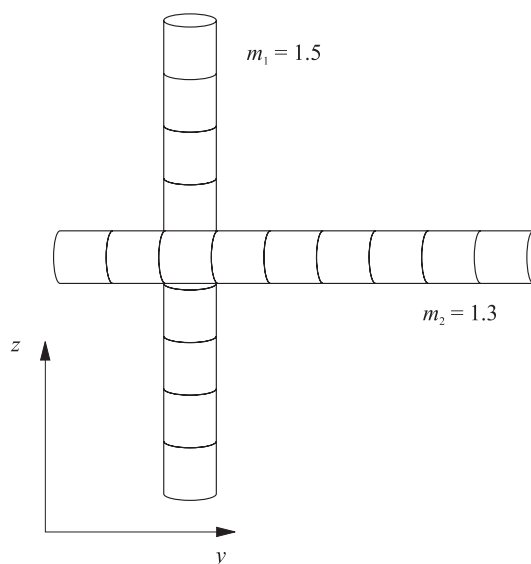


Fig. 7: Geometry of two attached fibres. Both fibres consist of 9 identical cylindrical elements with an aspect ratio of 1:1. The refractive indices are different for both fibres.

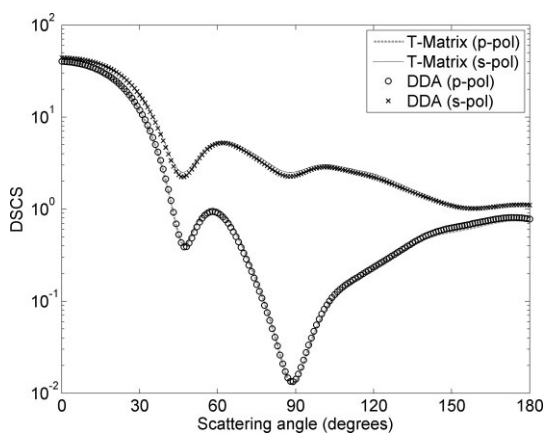


Fig. 8: DSCSs for two aggregated fibres with the size parameter $kd = 2.0$. The continuous curves show the DSCSs from **T**-matrix calculations. The crosses show the DSCSs by DDA calculations.

shown in Figure 9. It can be seen that for size parameters up to $kd = 2.0$ the RMS errors are quite low. The RMS error is increasing for values higher than $kd = 2.0$. This leads to unacceptable deviations in the computed DSCS. The computation time for the described simulations of the two attached fibres are summarized in Table 1. For the **T**-matrix method the computation time is multiplied by a factor of approximately eight when doubling the size parameter. The computation for the size parameter $kd = 4.0$ takes 520 seconds. The computation time of the DDSCAT program is nearly constant at 7 seconds for size parameters up to $kd = 2.0$ and is strongly increasing up to 153 seconds for the size parameter $kd = 4.0$.

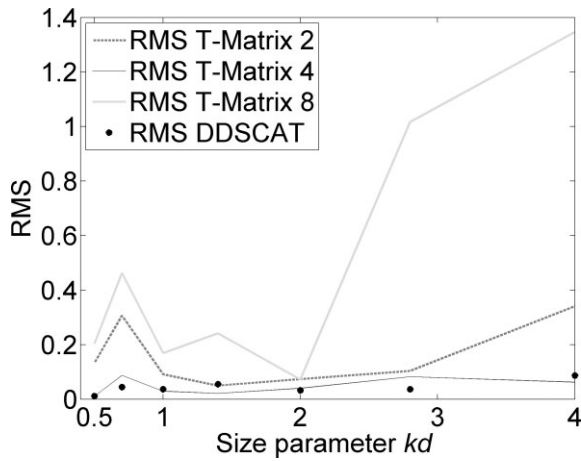


Fig. 9: RMS error between the **T**-matrix and the DDA computation for two aggregated fibres. The RMS error for p-polarization and for s-polarization shows strongly increasing values for $kd > 2$.

Table 1: Comparison of computation time between the **T**-matrix method and DDA for two attached fibres.

Computation	$kd = 1.0$	$kd = 1.4$	$kd = 2.0$	$kd = 2.8$	$kd = 4.0$
T -matrix	9s	28s	76s	265s	520s
DDA	7s	7s	8s	15s	153s

The maximum memory used during computation is presented in Table 2. The memory requirement during runtime of the computation is increasing for the **T**-matrix method up to a value of 315MB (megabyte). For DDSCAT computations the required memory is mainly dependent on the number of dipoles used. For the size parameter of $kd = 4.0$ the total memory required is 306MB. For smaller size parameters the memory required is fixed to 101MB. This is necessary because the number of dipoles must not fall under a value for which the shape is not correctly represented.

All computations were executed on a Workstation with two Quad-Core Xeon 64bit processors (Intel E5345, 2.33GHz) with a Linux 64 operating system. For both programs, **T**-matrix and DDSCAT, the Intel Fortran Compiler was used.

Table 2: Comparison of maximum memory usage during runtime between the **T**-matrix method and DDA for two attached fibres.

Max. memory used	$kd = 1.0$	$kd = 1.4$	$kd = 2.0$	$kd = 2.8$	$kd = 4.0$
T -matrix	37MB	60MB	131MB	242MB	315MB
DDA	101MB	101MB	101MB	101MB	306MB

7 Conclusion

A new method for computation of the **T**-matrix of aggregated fibres is presented. It is based on decomposing of a scattering particle into smaller units and a multiple scattering approach using the Null-Field Method with Discrete Sources (NFM-DS). By using decomposition of the scattering particles, the intersecting region of the circumscribing spheres is strongly reduced. This allows computation of scattering by aggregated particles like fibres or other non-spherical particles.

The final example of two attached fibres demonstrates good computational results up to a size parameter of $kd = 2.0$. This limit can not be generalized to other geometries, especially using more complex geometries like aggregated platelets, torus or helix shaped particles. In each case, a detailed analysis of the RMS error should be considered.

8 Acknowledgement

We would like to acknowledge support of this research by DFG (Deutsche Forschungsgemeinschaft).

9 Nomenclature

d	diameter of fibre
$\mathbf{e} = [a_v, b_v]^T$	expansion coefficients of the incident field
$\mathbf{E}_e, \mathbf{E}_s$	incident and scattered electric field
$\mathbf{H}_e, \mathbf{H}_s$	incident and scattered magnetic field
(\mathbf{e}, \mathbf{h})	surface current densities
g	Green function
k	wavenumber
l	length of fibre
$\{\mathbf{M}_v^{1,3}, \mathbf{N}_v^{1,3}\}$	vector spherical wave functions
m	refractive index
\mathbf{n}	normal vector
O	origin
r	radius of fibre
\mathbf{r}	position vector
$\mathcal{R}(-\gamma_1, -\beta_1, -a_1)$	rotation matrix
$\mathbf{s} = [f_v, g_v]^T$	expansion coefficients of the scattered field
S	particle surface
$\mathcal{S}_{10}^{\text{tr}}$	transformation matrix
$\mathcal{T}^{33}(-k_s \mathbf{r}_{01})$	translation matrix
\mathbf{T}	transition matrix
x, y, z	cartesian coordinates
a, β, γ	Euler angles
θ, φ	angular coordinates
ε	permittivity

λ	wavelength
μ	permeability
DDA	Discrete Dipole Approximation
DSCS = $ \mathbf{E}_{\text{sc}} ^2$	differential scattering cross section
NFM-DS	Null-Field Method with Discrete Sources

10 References

- [1] P. W. Barber, S. C. Hill, *Light Scattering by Particles: Computational Methods*. World Scientific, Singapore, **1990**.
- [2] M. I. Mishchenko, L. D. Travis, *T-matrix computations of light scattering by large spheroidal particles*. *Opt. Commun.* **1994**, *109*, 16–21.
- [3] H. Laitinen, K. Lumme, *T-Matrix method for general starshaped particles: first results*. *J. Quant. Spectrosc. Radiat. Transfer* **1998**, *60*, 325–334.
- [4] F. M. Kahnert, J. J. Stamnes, K. Stamnes, *Application of the extended boundary condition method to homogeneous particles with point-group symmetries*. *Appl. Opt.* **2001**, *40*, 3110–3123.
- [5] T. Wriedt, *Using T-Matrix Method for Light Scattering computations by Non-Axisymmetric Particles: Superellipsoids and Realistically Shaped Particles*. *Part. Part. Syst. Charact.* **2002**, *19*, 256–268.
- [6] A. Doicu, T. Wriedt, Y. Eremin, *Light Scattering by Systems of Particles. Null-Field Method with Discrete Sources – Theory and Programs*. Springer Verlag, Berlin, Heidelberg, New York, **2006**.
- [7] M. I. Mishchenko, G. Videen, V. A. Babenko, N. G. Khlebtsov, T. Wriedt, *T-matrix theory of electromagnetic scattering by particles and its applications: a comprehensive reference database*. *J. Quant. Spectrosc. Radiat. Transfer* **2004**, *88*, 357–406.
- [8] M. I. Mishchenko, G. Videen, V. A. Babenko, N. G. Khlebtsov, T. Wriedt, *Comprehensive T-matrix reference database: a 2004–2006 update*. *Journal of Quantitative Spectroscopy & Radiative Transfer* **2007**, *106*, 304–324.
- [9] S. Pulbere, T. Wriedt, *Light Scattering by Cylindrical Fibres with High Aspect Ratio Using the Null-Field Method with Discrete Sources*. *Part. Part. Syst. Charact.* **2004**, *21*, 213–218.
- [10] T. Wriedt, J. Hellmers, E. Eremina, R. Schuh, *Light scattering by single erythrocyte: Comparison of different methods*. *Journal of Quantitative Spectroscopy & Radiative Transfer* **2006**, *100*, 444–456.
- [11] T. Wriedt, *A Review of Elastic Light Scattering Theories*. *Part. Part. Syst. Charact.* **1998**, *15*, 67–74.
- [12] T. Wriedt, A. Doicu, *T-Matrix method for light scattering from particles on or near an infinite surface*, in *Light Scattering from Microstructures* (Eds.: F. Moreno, F. González), Springer, Berlin, **2000**, 113–132.
- [13] D. Ngo, G. Videen, R. Dalling, *Chaotic light scattering from a system of osculating, conducting spheres*. *Physics Letters* **1997**, *A 227*, 197–202.
- [14] B. T. Draine, P. J. Flatau, *User guide to the discrete dipole approximation code DDSCAT 6.1*. URL: <http://arxiv.org/abs/astro-ph/0409262> **2004**.
- [15] T. Wriedt, *Studies of light scattering by complex particles using the null-field method with discrete sources*, in *Light Scattering Reviews 2* (Ed.: A. A. Kokhanovsky), Springer Praxis, Berlin **2007**.
- [16] B. Peterson, S. Ström, *T-matrix for electromagnetic scattering from an arbitrary number of scatterers and representations of E(3)*. *Phys. Rev.* **1973**, *8*, 3661–3678.
- [17] B. Peterson, S. Ström, *Matrix formulation of acoustic scattering from an arbitrary number of scatterers*. *J. Acoust. Soc. Am.* **1974**, *56*, 771–780.
- [18] R. Schuh, *Arbitrary particle shape modelling in DDA and validation of simulation results*, in T. Wriedt, A. Hoekstra (Eds.): *Proceedings of the DDA – Workshop*, Institut für Werkstofftechnik, Bremen, 23. March **2007**, 22–24.